mathematics

MDPI

Article

Modelling of Interaction Dynamics of a Pathogen and Bio-Markers (Matrix Metalloproteinases) of Tissue Destruction in Pulmonary Tuberculosis

Anastasia I. Lavrova [1,2,*], Dilyara S. Esmedljaeva [2], Eugene B. Postnikov [3,*]

[1] Sophya Kovalevskaya North-West Mathematical Research Center, Immanuel Kant Baltic Federal University, Nevskogo St. 14, 236041 Kaliningrad, Russia
[2] Saint-Petersburg State Research Institute of Phthisiopulmonology, Ligovskiy Prospect 2-4, 194064 Saint Petersburg, Russia
[3] Theoretical Physics Department, Kursk State University, Radishcheva St. 33, 305000 Kursk, Russia
* Correspondence: anlavrova@kantiana.ru (A.I.L.).; postnikov@kursksu.ru (E.B.P.)

Abstract: Tuberculosis (TB) has a long history as a serious disease induced by its causative agent *Mycobacterium tuberculosis*. This pathogen manipulates the host's immune response, thereby stimulating inflammatory processes, which leads to an even greater imbalance of specific enzymes/inhibitors that contribute to tissue destruction. This work addresses a model consisting of two ordinary differential equations obtained by reducing a previously developed large-scale model describing lung damage, taking into account key metabolic pathways controlled by bacteria. The resulting system is explored as a dynamical system simulating the interaction between bio-markers (matrix metalloproteinases) of tissue destruction and the pathogen. In addition to the analysis of the mathematical model's features, we qualitatively compared the model dynamics with real clinical data and discussed their mutual correspondence.

Keywords: host–pathogen model; *M. tuberculosis*; nonlinear ODE; mathematical biophysics

MSC: 37N25; 92C45

Citation: Lavrova, A.I.; Esmedljaeva, D.S.; Postnikov, E.B. Modelling of Interaction Dynamics of a Pathogen and Bio-Markers (Matrix Metalloproteinases) of Tissue Destruction in Pulmonary Tuberculosis. *Mathematics* **2023**, *11*, 4522. https://doi.org/10.3390/math11214522

Academic Editor: Ricardo Lopez-Ruiz

Received: 15 October 2023
Revised: 29 October 2023
Accepted: 30 October 2023
Published: 2 November 2023

1. Introduction

A decade ago, the problem of exploring the host–pathogen interactions accompanying the development of tuberculosis was claimed as one of the crucial goals for exploration and modelling in this field [1]. Despite certain advances achieved during these years (see for review, e.g., [2–5]), the problem is far from a complete resolution.

Among the issues which induce the most active current interest, one can list the following. A variety of formation paths and outcomes of the tuberculosis granuloma is understood as governed by a complex proteomic network of interactions, among which the collagenase matrix metalloproteinase-1 (M_1) plays a valuable role, being included in multiple interactions [6]. The biochemical interactions of the components of the *M. tuberculosis* cell wall with the host's cell modulating inflammatory and immune responses [7] includes interactions that can play the role of potential drug targets [8]. The need for taking into account the complex of biochemical, biophysical and microbial drivers of the disease's development in the case of cavitary tuberculosis is highlighted in the review [9]. The search for biomarkers, which can be determined non-invasively, e.g., from blood samples, and can efficiently characterize the disease's development, monitor the effectiveness of anti-TB drugs, etc., is among the hot topics of research in this field [10,11].

Among such biomarkers, matrix metalloproteinases (MMPs) play a special role [12–14]. The primary role of these proteolytic enzymes consists of their participation in the degradation of the tissue's extracellular matrix induced by the action of *M. tuberculosis*. Among the

most valuable representatives of this family one can note collagenases (M_1 and M_8), stromelysin (M_3), and gelatinase (M_9). During the inflammatory process, the action of MMPs is also balanced by the tissue inhibitor of metalloproteinases (TIMP). What is important is that the respective processes lead to the change in the concentration of these substances not only locally in tissues but also in a partient's blood, which makes it possible to develop fast non-invasive diagnostic methods [15,16], predict treatment outcomes [17] and classify strains of *M. tuberculosis* respectively to their status of drug resistance [18,19].

A number of approaches to the computational models of pulmonary tuberculosis-related fibrosis processes are considered in the work [20]. They include discrete (metabolic network-based and agent-based) and continual (operating with systems of differential equations) models as well as hybrid ones. The multiscale models allow for connecting the dynamics of the concentration of characteristic metabolites with the macroscopic dynamics of the tissue components' structuring. Several existing models are especially devoted to the dynamics of matrix metalloproteinases in connection with bacterial burden and biophysical properties and transformations of the lung tissue's collagen. In particular, the authors of the work [21] operated with a system of ordinary differential equations consisting of the mass-balance-based equations for the MMPs and collagen's concentration supplied additionally with an equation stating the bacterial leakage. This system was focused on granuloma-related dynamical structuring. A more detailed ODE-based picture of the lesion formation as the generation and evolution of spherical "bubbles" is addressed in the work [22] but without taking into account the possible temporal evolution of MMP's and mycobacterial population explicitly. On the contrary, a population dynamics mathematical model for the bacterial burden inside of a lesion was developed in the work [23] respectively to different kinds of disease courses (granuloma, fibrocalcific form, etc.). The model, comprised of three ordinary differential equations built by the authors of the work [24], is devoted to the the activation of the inflammatory process, where MMPs are considered within a generalized variable, which takes into account complex pro-inflammatory mediators. The game-theoretical approach to the dynamics of a medium-size network of the host–pathogen interactions determined from the gene expressions (including those, which code MMPs) in samples taken from a cohort of patients was considered in the work [25]. Additionally, a differential-equation-based model for the macrophage proinflammatory response against *M. tuberculosis,* including granuloma's dynamics, among the factors of which MMP-9 was considered, was constructed and analysed in work [26].

Earlier [27], we proposed a multi-variable model characterising the principal scheme of interactions between the mycobacterial load and concentrations of the matrix metalloproteinases M_1, M_3, M_8 and M_9, the expression of their precursors (pMP), cytokines and the product and substrate of the lung-cavity-related tissues. Although this detailed model captures the principal features of the cavity formation and closing after treatment supplied with the auxiliary biochemical dynamics, its general dynamics cannot be analysed in detail due to the high multidimensionality of the model. Thus, the principal goal of the present work is in the formulation and analysis of a much more simplified system of ordinary differential equations able, notwithstanding, to capture the principal biochemical dynamics of the disease progress as the response to the dynamics of the intra-lung mycobacterial load.

2. Model

2.1. Model Statement

In constructing the simplified model, we relied on the full model developed by us earlier [27] but with slight modifications. While the previous study is focused more on the conditions of cavern formation or other forms of inflammation, in this study we are more interested in the dynamics of the pathogen and matrix metalloproteinases, whose over-activity leads to the destruction of lung tissue.

To construct a kinetic scheme for the activation of matrix metalloproteinase (see Figure 1), we considered the processes of pathogen activation of pro-enzymes, which leads to the over-expression of matrix metalloproteinases (MMPs). As in the previous study,

the set of reactions leading to M_1 overexpression was denoted by a single variable A. Since such processes ensure the survival and proliferation of *Mtb*, it is reasonable to assume the presence of positive feedback between A and *Mtb*. The pool of reactions responsible for suppressing M_1 synthesis was also summed up (variable I). As for the signalling pathway of cytokine activation by the pathogen, processes involving the activation or inhibition of MMPs, in particular M_1, have been considered (see Figure 1).

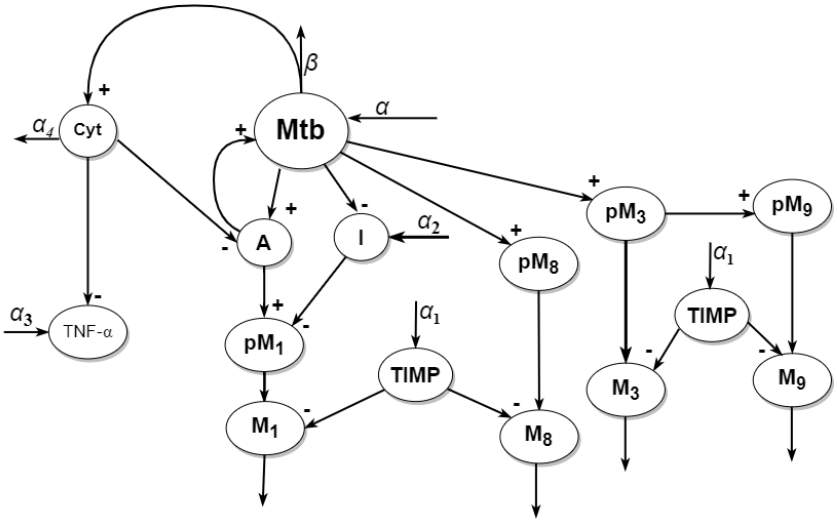

Figure 1. The kinetic scheme of processes resulting in the lung tissue destruction during TB, where α_i ($i = 1, 2, 3, 4$) are in- and out-fluxes of the metabolites; α, β determine pathogen reproduction and depletion due to treatment; Mtb—pathogen population; M_i ($i = 1, 3, 8, 9$)—matrix metalloproteinases/enzymes, involved in the destruction of lung tissue during the tuberculosis process; pM_i ($i = 1, 3, 8, 9$)—pro-matrix metalloproteinases/enzymes, activating M_i synthesis; TIMP—matrix metalloproteinase inhibitor; Cyt,TNF $-$ α denote key metabolites of immune reactions; A and I define a pool of reactions that activate and inhibit the overexpression (oversynthesis) of matrix metalloproteinase-1 (pM_1).

The system of equations describing the dynamics of the pathogen, as well as the metabolic pathways it governs within the framework of formal kinetics, will be as follows:

$$\frac{d[Mtb]}{dt} = \alpha - k_r[A][Mtb] - \beta[Mtb], \quad (1)$$

$$\frac{d[A]}{dt} = k_A[Mtb] - [A](\mu + mk_r[Mtb] + k_{AI}[Cyt]), \quad (2)$$

$$\frac{d[I]}{dt} = \alpha_2 - [I](k_{mtbI}[Mtb] + k_{outI}), \quad (3)$$

$$\frac{d[Cyt]}{dt} = k_{cyt}[Mtb] - \alpha_4[Cyt], \quad (4)$$

$$\frac{d[TNF]}{dt} = \alpha_3 - [TNF](k_{TNF}[Cyt] + k_{out}), \quad (5)$$

The synthesis of metalloproteinases (M_1, M_3, M_8, M_9) is conditioned by the expression of pro-MMPs (pM_1, pM_3, pM_8, pM_9). An inhibitor of MMPs, TIMP, can be also inhibited by Mtb components, but it has not yet been investigated in detail [12]. All reactions in the kinetic scheme were considered irreversible, and the outflow of enzymes from the environment was assumed to be very slow and therefore was not included in the system description.

Thus, we obtain the following set of kinetic reactions:

$$\frac{d[pM_1]}{dt} = \frac{\mu[A]}{[I]+[I_0]} - k_{pm_1}[pM1], \quad (6)$$

$$\frac{d[pM_3]}{dt} = k_{mtb_3}[Mtb] - k_{pm_3}[pM_3], \quad (7)$$

$$\frac{d[pM_8]}{dt} = k_{mtb_8}[Mtb] - k_{pm_8}[pM_8], \quad (8)$$

$$\frac{d[pM_9]}{dt} = k_{mtb_9}[Mtb] - k_{pm_9}[pM_9], \quad (9)$$

$$\frac{d[M_1]}{dt} = k_{pm_1}[pM_1] - k_{TIMP}[M_1][TIMP], \quad (10)$$

$$\frac{d[M_3]}{dt} = k_{pm_3}[pM_3] - k_{TIMP}[M_3][TIMP], \quad (11)$$

$$\frac{d[M_8]}{dt} = k_{pm_8}[pM_8] - k_{TIMP}[M_8][TIMP], \quad (12)$$

$$\frac{d[M_9]}{dt} = k_{pm_9}[pM_9] - k_{TIMP}[M_9][TIMP], \quad (13)$$

$$\frac{d[TIMP]}{dt} = \alpha_1 - [TIMP](k_{mtbT}[Mtb] + k_{TIMP}\sum[Mi] + k_{outT}), \quad (14)$$

where $\sum_{i=1,3,8,9}[M_i] = [M_1]+[M_3]+[M_8]+[M_9]$ and the respective units conventionally used in biochemical and clinical practice are listed in Table 1.

Table 1. Units of dimensional variables and parameters in Equations (1)–(14).

Variables		**Units**	
Metabolite concentrations *		ng mL^{-1}	
$[Mtb]$		cfu mL^{-1}	
t		d **	
α	mL^{-1}d^{-1}cfu	k_{outT}	d^{-1}
k_r	ng^{-1}d^{-1}mL	k_{pm_1}	d^{-1}
β	d^{-1}	k_{pm_3} k_{pm_8}	d^{-1}
k_A	cfu^{-1}d^{-1}ng	k_{pm_9}	d^{-1}
μ	ng mL^{-1}d^{-1}	k_{mtb_3}	cfu^{-1}d^{-1}ng
m-factor	cfu^{-1}ng	k_{mtb_8}	cfu^{-1}d^{-1}ng
k_{AI}	ng^{-1}d^{-1}mL	k_{mtb_9}	cfu^{-1}d^{-1}ng
α_2	mL^{-1}d^{-1}ng	k_{mtbt}	cfu^{-1}d^{-1}ng
k_{mtbI}	cfu^{-1}d^{-1}mL	k_I	ng^{-1}d^{-1}mL
k_{cyt}	cfu^{-1}d^{-1}ng	k_{TIMP}	ng^{-1}d^{-1}mL
α_6	d^{-1}	α_1	mL^{-1}d^{-1}ng
α_3	mL^{-1}d^{-1}ng		
k_{TNF}	ng^{-1}d^{-1}mL		
k_{out}	d^{-1}		
k_{outI}	d^{-1}		

* $[A]$, $[I]$, $[Cyt]$, $[TNF]$, $[pM_1]$, $[pM_3]$, $[pM_8]$, $[pM_9]$, $[M_1]$, $pM_3]$, $[M_8]$, $[M_9]$, $[TIMP]$; ** days.

It should be noted that the dependence of pro matrix metalloproteinase-1 (pM_1) on the pools of activating (A) and inhibiting reactions (I) (see Equation (6)) was taken into account due to the fact that pathogen activation of the pool leads to over-synthesis of pM_1. In the absence of a pathogen, pool A is not active, and the pool of inhibiting reactions is activated, resulting in a normal level of pM_1. The variable I_0 represents the main level of inhibitory reactions in the host cell.

2.2. Model Reduction

According to clinical data, the concentration of the immune system metabolites TNF and Cyt remains high (increasing by 10^4 times) and practically constant during both the inflammatory process and the first phase of treatment, and the concentration of the inhibitor $TIMP$ remains constant too. In the experiment, the total concentration $pM_i + M_i$ was measured; therefore, the system of Equations (6)–(13) can be reduced, assuming for simplicity that the concentration of pro-enzymes varies in proportion to the concentration of the enzyme; i.e., $pM_i = \xi M_i$, and therefore $pM_i + M_i = (1 + \xi)M_i$. Thus, we obtain the expressions for the concentrations of $MMPs$, $TIMP$, TNF and Cyt, while the kinetic constants will be normalized to the coefficient $1 + \xi$:

$$\frac{d[M_1]}{dt} = \frac{\tilde{\mu}[A]}{[I] + [I_0]} - \tilde{k}_{TIMP}[M_1][TIMP], \tag{15}$$

$$\frac{d[M_3]}{dt} = \tilde{k}_{mtb_3}[Mtb] - \tilde{k}_{TIMP}[M_3][TIMP], \tag{16}$$

$$\frac{d[M_8]}{dt} = \tilde{k}_{mtb_8}[Mtb] - \tilde{k}_{TIMP}[M_8][TIMP], \tag{17}$$

$$\frac{d[M_9]}{dt} = \tilde{k}_{mtb_9}[Mtb] - \tilde{k}_{TIMP}[M_9][TIMP]. \tag{18}$$

Here, $\widetilde{k_I} = k_I\xi/(1 + \xi)$, and the rest of the terms supplied with tildes are equal to the respective quantities without tildes simply divided by $1 + \xi$.

$$[Cyt] = \frac{k_{cyt}}{\alpha_4}[Mtb] = \gamma_2[Mtb], \tag{19}$$

$$[TNF] = \frac{\alpha_3}{k_{TNF}[Cyt] + k_{out}} = \frac{\gamma_1}{\gamma_3[Mtb] + 1}, \tag{20}$$

$$[TIMP] = \frac{\alpha_1}{k_{mtbT}[Mtb] + k_{TIMP}\sum[M_i] + k_{outT}}, \tag{21}$$

where $\gamma_1 = \frac{\alpha_3}{k_{out}}$ and $\gamma_3 = \gamma_2\frac{k_{TNF}}{k_{out}}$.

It should be noted that the dynamics of the pathogen and metalloproteinases, as well as their influence on each other, are of interest to us, and therefore we will not consider the obtained functions of the immune metabolites (19) and (20). After dimensionality reduction of the system and substitution of the expression (21) into the Equations (15)–(18), the following system for dimensionless variables and parameters was obtained:

$$\frac{dMtb}{d\tau} = \alpha_d + Mtb(A - \beta_d), \tag{22}$$

$$\frac{dA}{d\tau} = Mtb - A(\nu + Mtb\gamma_d), \tag{23}$$

$$\frac{dI}{d\tau} = \alpha_{2d} - I(Mtb - k_{outI_d}), \tag{24}$$

$$\frac{dM_1}{d\tau} = \frac{\nu_1 A}{I + 1} - M_1\tilde{F}, \tag{25}$$

$$\frac{dM_3}{d\tau} = k_3 Mtb - M_3\tilde{F}, \tag{26}$$

$$\frac{dM_8}{d\tau} = k_8 Mtb - M_8\tilde{F}, \tag{27}$$

$$\frac{dM_9}{d\tau} = k_9 Mtb - M_9\tilde{F}. \tag{28}$$

where

$$\tilde{F} = \frac{\alpha_{1_d}}{\beta_1[Mtb] + \beta_2\sum[M_i] + 1}$$

and all new dimensionless parameters are combinations of dimensional parameters and concentrations of metabolites: $\alpha_d = \frac{\alpha t_0}{Mtb_0}$, $\beta_d = \beta_0 t_0$, $\nu = \mu t_0$, $\gamma_d = mk_r Mtb_0 t_0 + k_{AI}\gamma_2 Mtb_0 t_0$, $\alpha_{2d} = \frac{\alpha_2 t_0}{I_0}$, $\nu_1 = \frac{\tilde{\mu} t_0 A_0}{\sum [M_{i0}] I_0}$, $k_3 = \frac{\tilde{k}_{mtb_3} Mtb_0 t_0}{\sum M_{i_0}}$, $k_8 = \frac{\tilde{k}_{mtb_8} Mtb_0 t_0}{\sum M_{i_0}}$, $k_9 = \frac{\tilde{k}_{mtb_9} Mtb_0 t_0}{\sum M_{i_0}}$, $\alpha_{1_d} = \frac{\alpha_1 \tilde{k}_{TIMP} t_0}{k_{outT}}$, $\beta_1 = \frac{k_T Mtb_0}{k_{outT}}$, $\beta_2 = \frac{\tilde{k}_{TIMP}(1+\xi)\sum M_{i_0}}{k_{outT}}$.

Since by "activator" and "inhibitor", we mean a pool of reactions, and assuming (for simplicity) that this pool is in equilibrium, it is reasonable to equalize $\frac{d[A]}{d\tau}$ and $\frac{d[I]}{d\tau}$ to zero. Assuming Ik_{outId} is very slow ($\approx$0), and substituting the obtained expressions for $[A]$ and $[I]$ into the rest of the equations, we obtain:

$$\frac{dMtb}{d\tau} = \alpha_d + Mtb\left(\frac{Mtb}{\nu + Mtb\gamma_d} - \beta_d\right), \tag{29}$$

$$\frac{dM_1}{d\tau} = \frac{\nu_1 Mtb^2}{(\nu + Mtb\gamma_d)(\alpha_{2d} + MTb)} - [M_1][\tilde{F}], \tag{30}$$

$$\frac{dM_3}{d\tau} = k_3 Mtb - M_3\tilde{F}, \tag{31}$$

$$\frac{dM_8}{d\tau} = k_8 Mtb - M_8\tilde{F}, \tag{32}$$

$$\frac{dM_9}{d\tau} = k_9 Mtb - M_9\tilde{F}. \tag{33}$$

As the last step, we sum up Equations (30)–(33) by substituting the expression for $\tilde{F}$ and re-designating the constants. The final system will be as follows:

$$\frac{dMtb}{d\tau} = \frac{\gamma^{-1} Mtb^2}{Mtb + \nu/\gamma} - \beta Mtb + \alpha \tag{34}$$

$$\frac{dM}{d\tau} = -\frac{\gamma_1 M}{\beta_m M + (Mtb + \beta_0)} + \left(\frac{\gamma^{-1} Mtb}{Mtb} + \nu/\gamma\right)\left(\frac{\nu_1 Mtb}{Mtb + \alpha_2}\right) + Mtb\nu_{\text{sum}} \tag{35}$$

where $M = \sum M_i$, $\alpha_{2d} = \alpha_2$, $\gamma_{2d} = \gamma_2$, $\gamma_1 = \alpha_{1d}/\beta_1$, $\alpha_d = \alpha$, $\beta_d = \beta$, $\beta_m = \beta_1/\beta_2$, $\beta_0 = 1/\beta_1$, $\nu_{sum} = k_3 + k_8 + k_9$.

Although it eliminated the possibility of tracing the dynamics of multiple intermediate biochemical reagents, such as pro-enzymes, metabolites of immune reactions, etc., Equation (35) provide an advantage in both mathematical and biophysical senses. Two nonlinear equations allow for building simple low-dimensional algebraic equations, the solution of which defines stationary states and asymptotic regimes. Moreover, they can be easily illustrated and analysed graphically, which is virtually impossible for the original system of 14 variables and dozens of constants. This also provides an opportunity to choose and adjust the remaining constants or their combinations in such a way that the simulated time series reproduce experimental ones. Note that the concentration of metalloproteinases governed by Equation (35) can be experimentally measured.

For further simulations, which require numerical solving of the system (34) and (35), we used the MATLAB 2014b, applying its standard ODE solver `ode45`, which realises an explicit Runge–Kutta (4,5) formula with the Dormand–Prince pair.

3. Results

It should be pointed out that the system (34) and (35) represents the unidirectional coupling. This means that Equation (34) can be considered as an isolated equation describing the population dynamics of *M. tuberculosis* in lungs. Its solution stated as a function of time plays the role of perturbation acting on the biochemical dynamics of the metalloproteinase concentration defined by Equation (35). At the same time, this governing action is not a trivial influx since there is not only a nonlinear influx (the second and the third terms in Equation (35) but also a parameter modification of the first term containing the

dependence on the metalloproteinase concentration. Certainly, due to the high nonlinearity of Equation (35), this nonhomogeneity of the equation gives a non-trivial response.

Note that Equation (34), which determines the population growth of *M. tuberculosis*, has the formal form coinciding with the so-called Bazykin model with external influx in population dynamics. The dynamical properties of this this model are well studied, see e.g., [28], whence we will not focus on them in detail but provide the basic characteristic parameters useful for the further consideration of the full dynamics.

Note that it is more demonstrable to consider the reduced mycobacterial population and the reduced time defined as $Mtb' = \beta Mtb$ and $\tau' = \beta\tau$, respectively. This allows a more simple representation of Equation (34) in the form

$$\frac{dMtb'}{d\tau'} = \frac{\left(Mtb'\right)^2}{\gamma' Mtb' + \nu'} - Mtb' + \alpha', \tag{36}$$

where the reduced parameters $\alpha' = \alpha/\beta$, $\gamma' = \beta\gamma$, $\nu' = \beta^2\nu$ are introduced.

There are two possible cases related to the influx of mycobacteria. Medically, the first one relates to the the patient suffering from tuberculosis but isolated from the external bacterial load, i.e., $\alpha' = 0$. In this case, the Equation (34) has two simple stationary points corresponding to $dMtb'/d\tau' = 0$. The first one is the trivial unstable equilibrium of the population's absence, $\left(Mtb'\right)_s = 0$. The second one is defined by the simple relation

$$\left(Mtb'\right)_s = \frac{\nu'}{1-\gamma'}. \tag{37}$$

It is important that the population density always can be only non-negative. Thus, Equation (37) directly implies the strict restriction $\gamma' \leq 1$, or, in the original notation, $\beta\gamma \leq 1$. Figure 2A illustrates the distribution of non-negative $\left(M'_{tb}\right)'_s s$ when they exist. Note that the original notation of parameters and the population density are used there as explicit combinations.

When $\alpha' \neq 0$, the conditions for the stationary state read as

$$\left(Mtb'\right)_s = \frac{(\nu' - \alpha'\gamma') \pm \sqrt{(\nu' - \alpha'\gamma')^2 - 4(1-\gamma')\alpha'\nu'}}{2(1-\gamma')}. \tag{38}$$

The biological sense requires that the realistic steady state should be non-negative, $\left(Mtb'\right)_s > 0$ and real-valued, i.e., $(\nu' - \alpha'\gamma')^2 - 4(1-\gamma')\alpha'\nu' > 0$. Since the third parameter, α', is added, the 2D colour map plot cannot be drawn. For this reason, Figure 2B illustrates non-negative real values of the stationary states calculated via Equation (38) as a superposition of two sets of countour plots differing by colour. The first one is for $\alpha' \equiv \alpha/\beta = 0.1$, and the second one is plotted for $\alpha' \equiv \alpha/\beta = 1$. One can see that the introduction of the bacterial influx changes the behaviour of the boundary existence of the equilibria, especially for small values of the small decay rates β'.

Thus, the principal features of the built reduced model (34) and (35) are contained in Equation (35). Its form indicates that it belongs to the class of kinetic equations of nonlinear response theory [29]. It is worth noting that in contrast to the case of linear inhomogeneous differential equations, the explicit separation of solution in free and induced responses is impossible in this case as is an analytical solution for such a complex influx term.

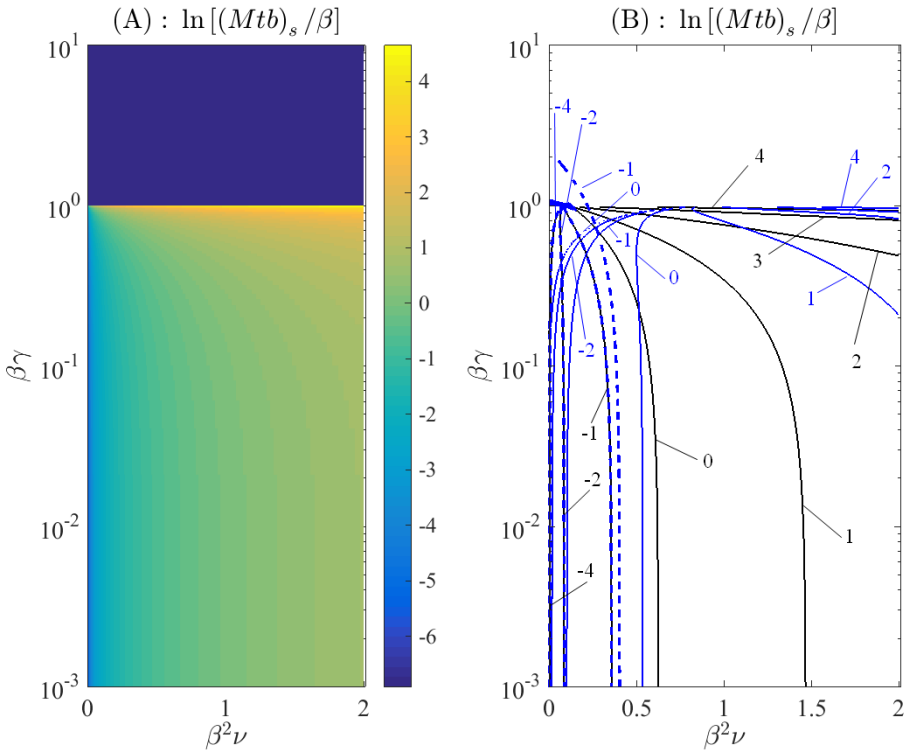

Figure 2. Parametric plots of non-trivial stationary states for Equation (36) representing logarithms of their values, where they exist. (**A**) The case $\alpha = 0$, dark blue region in the upper part ($\beta\gamma > 1$), depicts non-existence of such states. (**B**) Example contour plots for two cases of Equation (38): $\alpha = 0.1$ (black contours) and $\alpha = 1$ (blue contours). Solid and dashed lines correspond to two branches of the solution (when they exist).

However, several qualitative and quantitative conclusions are available. First of all, it should be stressed that the only term that contains M in the right-hand side of Equation (35) is always non-positive since $M \geq 0$, $Mtb \geq 0$ and all constant parameters are positive. This means that the homogeneous part of the differential equation describes a nonlinear decay whereby, for $Mtb \to 0$ and $M \to 0$, there is no maintaining the constant level of metalloproteinases in the considered model. In general, $M \neq 0$ is in the healthy state, but here we consider not a general case but the situation of a patient's diseased state only as controlled by the bacterial load. This load is supported by the second and the third terms in the right-hand side of Equation (35). They contain the value of Mtb considered above as solutions of an independent Equation (34).

Regarding this, when its parameters do not allow existence of a non-trivial equilibrium, $Mtb \to \infty$ for $\tau \to \infty$, the divergent sum of the last two terms of the considered inhomogeneous equation

$$\left(\frac{\gamma^{-1}M_{tb}}{M_{tb}+\nu/\gamma}\right)\left(\frac{\nu_1 M_{tb}}{M_{tb}+\alpha_2}\right)+M_{tb}\nu_{sum}\Big|_{Mtb\to\infty} \to \gamma^{-1}\nu_1 + M_{tb}\nu_{sum} \to \infty$$

induce the divergence of M too. The first term

$$-\frac{\gamma_1 M}{\beta_m M + (M_{tb}+\beta_0)}$$

cannot compensate this growth since it is limited by a constant from above: the denominator, which contains the weighted sum of the infinitely growing M and Mtb will be at least not smaller than the numerator, which contains M.

On the other hand, when the parameters of Equation (34) allow the existence of a non-trivial stationary solution ($(Mtb)_s$), it can be substituted in Equation (35) for sufficiently large time due to the independence of Equation (34) from Equation (35). In this case, the stationary non-zero solution M_s for Equation (35) defined by $dM/d\tau = 0$ ($Mtb = (Mtb)_s = \text{const}$) can exist and is given (if it exists) by

$$M_s = \frac{((Mtb)_s + \beta_0)\left[\left(\frac{\gamma^{-1}(Mtb)_s}{(tb)_s+\nu/\gamma}\right)\left(\frac{\nu_1(Mtb)_s}{(Mtb)_s+\alpha_2}\right) + (M_{tb})_s\nu_{\text{sum}}\right]}{\gamma_1 - \beta_m\left[\left(\frac{\gamma^{-1}(Mtb)_s}{(Mtb)_s+\nu/\gamma}\right)\left(\frac{\nu_1(Mtb)_s}{(Mtb)_s+\alpha_2}\right) + (Mtb)_s\nu_{\text{sum}}\right]}. \quad (39)$$

The nominator of Equation (39) is always positive, which implies that there is no equilibrium state $M_s = 0$ when $(Mtb)_s$ is finite. On the contrary, the denominator contains a difference of two positive quantities and diminishes with growing $(Mtb)_s$. Therefore, the situation of the denominator equal to less than zero can emerge in the case of a sufficiently large amount of active mycobacteria. It is the situation of an absence of the non-trivial equilibrium asymptotic stationary state for the concentration of metalloproteinases. The divergence of their concentration means that the bacterial load is too high and a patient's organism cannot defeat the disease. For the case of a finite positive denominator of Equation (39), a solution for the differential Equation (35) tends asymptotically to the finite stationary concentration given by Equation (39).

Dynamics of Matrix Metalloproteinases

To test whether the considered model represents the qualitative/semi-qualitative dynamics of the temporal evolution of the concentration of metalloproteinases, we use the real clinical data obtained during the longitudinal study in the Saint-Petersburg State Research Institute of Phthisiopulmonology. Thirteen patients with bacteriologically confirmed diagnosis of tuberculosis were examined, with an average age of 40.09 $\pm$ 3.05 years, who were undergoing treatment in a hospital between 2010 and 2020. Among the tuberculosis patients, infiltrative process was detected in 80% of cases, while 20% were associated with fibro-cavitary lesions. Serum biochemical analysis (from which matrix metalloproteinases are isolated) was performed four times: before and after 2, 4, and 6 months of intensive phase therapy. The small sample size can be explained by the fact that blood for matrix metalloproteinase measurement is usually taken before therapy, and it is difficult to organize regular testing every two months during treatment in a clinic. All raw data are given in the Supplementary Materials.

Figure 3 illustrates the median values (markers) for two sets of patients. The first one consists of those who suffer from fibro-cavernous (FCT) tuberculosis, and the second one corresponds to the case of infiltrative lung tuberculosis. Since the total sample contains data without gaps for 13 patients only, the plots provide rather limited statistics. The error bars are chosen in such a way that the values of quantiles correspond to the standard deviation of data satisfying the normal distribution. However, the amount of data is too small to consider parametric statistics, and the non-asymmetric quantal deviations are preferable in this case.

It can be seen (Figure 3) that for the major metalloproteinases, such as M_1, M_8 and M_9, the dynamics show a peak at 2 months (M_8) or 4 months (M_1, M_9), with only M_3 remaining near normal levels, which is generally consistent with clinical data [15]. It can also be observed that enzyme concentrations do not return to normal values after the intensive phase of therapy, especially in cases of fibro-cavernous tuberculosis. When studying the model dynamics of total metalloproteinase concentration (see Figure 4), a peak was also observed at high initial concentrations of Mtb (Figure 4A,B); however, the rate of decline towards steady state is regulated by the parameter gamma1 (see Equation (35)), with higher values leading to a faster decline in total concentration. It should be noted that the maximum increase in metalloproteinases occurs with a delay relative to the peak population of mycobacteria. This fact can be explained by the fact that the initiation

of processes leading to abnormal synthesis of matrix metalloproteinases occurs with a delay, when the pathogen has accumulated sufficiently in the tissue and restarts metabolic processes necessary for its reproduction.

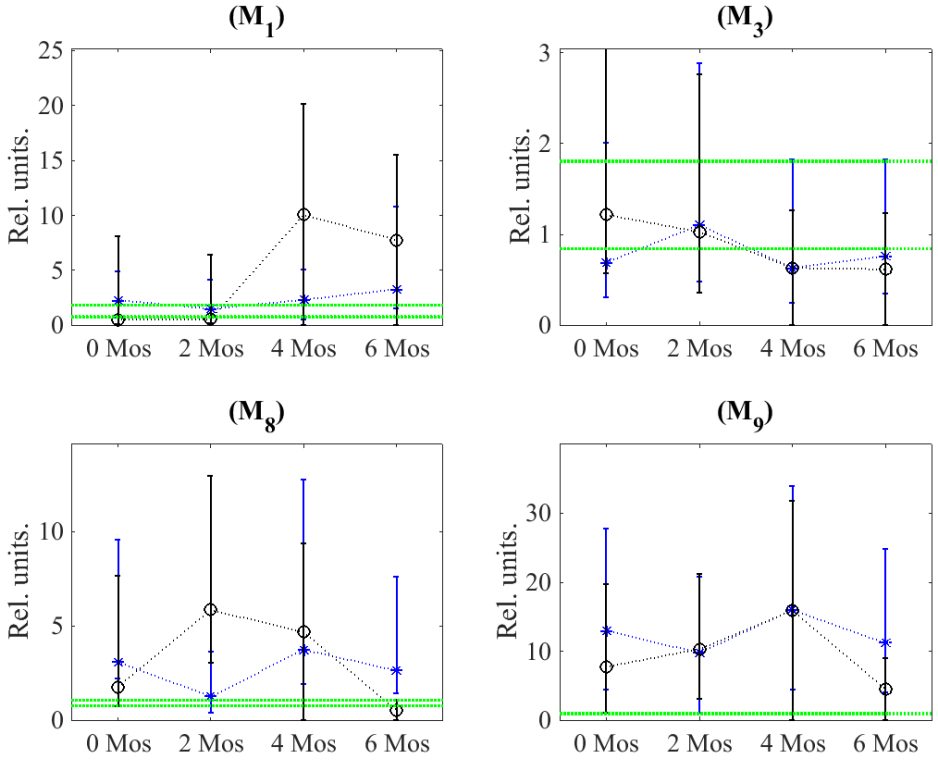

Figure 3. Dynamics of four types of matrix metalloproteinases measured with two-month time intervals (sub-panel names, M_1, M_3, M_8, M_9, correspond to their abbreviations). Circles and asterisks denote the medians of concentrations normed on healthy people's median levels for the cases of fibro-cavernous (FCT) and infiltrative lung tuberculosis, respectively (the connective dotted lines are added for visual guidance); error bars show 0.32 and 0.68 quantiles. The horizontal green dotted lines mark 0.32 and 0.68 quantiles for the case of healthy people (the data from the work [15], published under a Creative Commons licence, are used).

In principle, the parameter γ_1, which is primarily responsible for the rate of efflux of M (as well as the first negative term in the equation), may correspond to an increase in immunological and metabolic control [30] during intensive therapy, which may lead to blockade of over-synthesis of MMPs and an increase in tissue inhibitor TIMP of the metalloproteinases with an unchanged population of mycobacteria. However, in severe cases of FCT tuberculosis, this control mechanism does not work, resulting in constantly high concentrations of metalloproteinases, as shown in Figures 3 for M_1 and M_9 and 4C.

In the case of infiltrative tuberculosis (see Figure 3), the overall concentration of all metalloproteinases mainly fluctuates around the normal level, except for M_9. In the model, small values are achieved by reducing the initial population value of *Mtb* by approximately 20 times, as shown in Figure 4D.

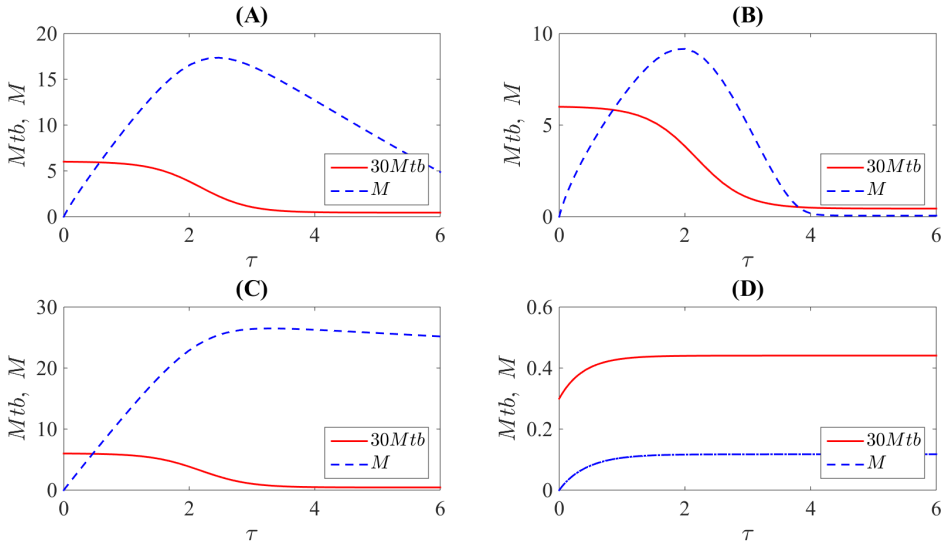

Figure 4. Model dynamics of MMP total concentration (M) and Mtb population in dependence on the initial population of pathogen and parameter γ_1. (**A**) Concentration dynamics of metalloprotinases with slow decay to steady state: $\gamma_1 = 4$, $Mtb_0 = 0.2$. (**B**) Concentration dynamics of metalloprotinases at possible immonological or metabolical control: $\gamma_1 = 8$, $Mtb_0 = 0.2$. (**C**) Monotonically increasing dynamics of metalloproteinase concentrations followed by saturation: $\gamma_1 = 0.9$, $Mtb_0 = 0.2$. (**D**) Dependence of matrix metalloproteinase dynamics on initial small pathogen population: $\gamma_1 = 4$, $Mtb_0 = 0.01$. The rest of the model parameters: $\alpha = 0.041$, $\beta = 3$, $\gamma = 0.009$, $\nu = 0.07$, $\nu_1 = 5$, $\nu_{sum} = 5$, $\alpha_2 = 0.02$, $\beta_m = 0.8$, $\beta_0 = 0.8$

4. Discussion

Equation (34) under conditions of the absence of the external influx α) exactly coincides with the Bazykin equation [28]:

$$\dot{x} = \frac{bx^2}{x+N} - dx, \tag{40}$$

which was derived from the population growth law $\dot{x} = b(x)x - dx$, where $b(x) = bx/(x+N)$ is the functional response and d is the mortality coefficient. Originally, Equation (40) related to the growth of the total population x for the case of biparental reproduction with different temporal breeding behaviour: either permanent (males) or with periods for which they are excluded from breeding opportunities (females).

In our case of asexual bacterial reproduction, Equation (34) has another interpretation. When Equation (34) is rewritten in the form

$$\frac{dMtb}{d\tau} = \gamma^{-1}\frac{\gamma Mtb}{\gamma Mtb + \nu}Mtb - \beta Mtb + \alpha \tag{41}$$

and $\gamma Mtb = S$ is denoted and taken as a substrate, the resulting form

$$\frac{dMtb}{d\tau} = \gamma^{-1}\frac{S}{S+\nu}Mtb - \beta Mtb + \alpha, \tag{42}$$

then Equation (42) coincides with the classic population growth equation with the substrate utilised for the Holling II functional response.

From this point of view, mycobacteria themselves prepare the substrate S required for their efficient reproduction acting on the lung tissue as

$$\frac{dS}{d\tau} = \gamma Mtb - S. \tag{43}$$

The second term in the right-hand side of Equation (43) indicates the substrate required for the multiplication of mycobacteria is "self-healing" with the unit rate. The first term corresponds to the activation of this substrate by mycobacteria. If these coexisting precesses are fast, i.e., $dS/d\tau \cong 0$, then the algebraic equation $\gamma Mtb - S = 0$ gives the equilibrium condition $S = \gamma Mtb$.

It is worth noting that such effects of substrates modified by a product are known for a range of population dynamics processes leading to growth faster than the exponential one. First of all, it is the seminal Kremer's demographic model [31]. It operates with the human population n growing accordingly to the Verhulst equation $\dot{n} = r_1 n(1 - n/K)$ where the stationary state $n = K$ is determined by the level of technological development. At the same time, the change of this technological level is a slow process, which also depends on the current population size as $\dot{K} = r_2 nK$. As a result, hyperbolic growth, satisfying the equation $\dot{n} = r_2 n^2$, is observed. The second example is the Markov–Korotayev model of the hyperbolic growth of phanerozoic marine biodiversity [32], which mathematically resembles Kremer's model but has a bioecological interpretation: species can change biogeocoenosis that leads to the emergence of new ecological niches and, as a result, to the hyperbolic growth of biodiversity.

The Holling II type of the functional response included in Equation (35) also has a direct interpretation in terms of Holling's original arguments [33], which address the time required for searching a nutrient substrate. In the considered situation, the density of such mycobacterial inhabited foci is given by γMtb. The spreading mycobacteria reach these substrate-rich foci, their density Mtb grows with the characteristic time ν^{-1} and acts as the source for the further spread. However, a delay defined by the growth rate ν emerges before the subsequent spread.

In the case of low mycobacterial density ($\gamma Mtb << \nu$), the first term in Equation (35) gives the quadratic growth speed:

$$\frac{\gamma Mtb}{\gamma Mtb + \nu} Mtb \approx \frac{\gamma Mtb^2}{\nu}$$

since mycobacteria need some time for the substrate modification and hyperbolic growth conditions discussed above to occur. Foe the high bacterial contamination ($\gamma M_{tb} >> \nu$), the extensive area of the lung tissue plays the role of such a substrate:

$$\frac{\gamma Mtb}{\gamma Mtb + \nu} Mtb \approx Mtb,$$

and this terms reduces to the Malthusian one for an averagely uniform constant substrate.

Now, let us discuss Equation (35), which also contains fractional–rational functions that allow an interpretation from the point of view of generalized chemical kinetics. Such an interpretation refers to the Langmuir–Hinshelwood mechanism, which gives the mathematical expression close to the Holling II population functional response and the Michalis–Menten enzyme–substrate kinetics, see [34]. This mechanism describes the reaction between reagents in a solution when they are captured by a surface covered by a catalyst.

Within this interpretation, it follows from the first term in Equation (35) that the amount of metalloproteinases decreases when they are cached by a binding surface and the binding rate depends on the presence of mycobacteria. The second term, which is stated as a product, gives the rate of synthesis of metalloproteinases on the catalysing surface absorbing mycobacteria. The mentioned product is a typical feature of the Langmuir–Hinshelwood process, when there are two binding centres with different activity (this difference is quantified by the different terms $\nu/\gamma$and α_2), see [35]. Finally, the last term in Equation (35) is a simple non-catalysed reaction.

5. Conclusions

To summarise, this work presents a model describing the interaction of the pathogen (*M. tuberculosis*) and the main bio-markers (matrix metalloproteinases) of lung tissue destruction during tuberculosis inflammation. The main focus of its reduced version is on the variables that are easily measured in real clinical studies: the amount of mycobacteria and the concentration of biochemical biomarkers called metalloproteinases. The remaining auxiliary processes are combined into dimensionless constants, making it easier to adjust them based on mathematical analysis of potential dynamic patterns and comparison with biomarkers obtained from healthy individuals serving as the reference group. Thus, to qualitatively compare the model dynamics with real data, we used clinical data obtained from the Institute of Phtisiopulmonology. We examined the dynamics of marker concentrations in various forms of tuberculosis, including monotonous growth with progression and bell-shaped dynamics. We showed that the multiplication of mycobacteria in the lungs can be explained by the dynamic behaviour described, in particular, by the Holling model, where population growth is determined by the search for a "convenient" substrate (lung tissue) with a time delay for the reproduction in a chosen focus.

Supplementary Materials: The following supporting information can be downloaded at: https://www.mdpi.com/article/10.3390/math11214522/s1, Table S1: diagnosis (initial), diagnosis (final), observation month, biomarker concentration for all patients.

Author Contributions: Conceptualization, A.I.L.; methodology, A.I.L. and E.B.P.; software, E.B.P. and A.I.L.; formal analysis, E.B.P. and A.I.L.; investigation, A.I.L., D.S.E. and E.B.P.; resources, D.S.E.; data curation, E.B.P.; writing—original draft preparation, E.B.P. and A.I.L.; writing—review and editing, A.I.L.; visualization, E.B.P.; supervision, A.I.L. and E.B.P.; funding acquisition, A.I.L. All authors have read and agreed to the published version of the manuscript.

Funding: A.I.L. was supported by the Project of the State Assignment of the Ministry of Education and Science of the Russian Federation no. 075-02-2023-934.

Informed Consent Statement: Informed consent was obtained from all subjects involved in the study.

Data Availability Statement: The anonymised data on the bimomthly dynamics concentration of matrix metalloproteinases in samples taken from patients suffering from lung tuberculosis are provided in the Supplementary Materials.

Conflicts of Interest: The authors declare no conflict of interest.

References

1. Pieters, J.; McKinney, J.D. (Eds.) *Pathogenesis of Mycobacterium tuberculosis and Its Interaction with the Host Organism*; Springer: Berlin/Heidelberg, Germany, 2013.
2. Kirschner, D.; Pienaar, E.; Marino, S.; Linderman, J.J. A review of computational and mathematical modeling contributions to our understanding of Mycobacterium tuberculosis within-host infection and treatment. *Curr. Opin. Syst. Biol.* **2017**, *3*, 170–185. [CrossRef] [PubMed]
3. Cadena, A.M.; Fortune, S.M.; Flynn, J.L. Heterogeneity in tuberculosis. *Nat. Rev. Immunol.* **2017**, *17*, 691–702. [CrossRef] [PubMed]
4. Magombedze, G.; Marino, S. Mathematical and computational approaches in understanding the immunobiology of granulomatous diseases. *Curr. Opin. Syst. Biol.* **2018**, *12*, 1–11. [CrossRef]
5. Vlazaki, M.; Huber, J.; Restif, O. Integrating mathematical models with experimental data to investigate the within-host dynamics of bacterial infections. *Pathog. Dis.* **2019**, *77*, ftaa001. [CrossRef] [PubMed]
6. Elkington, P.; Polak, M.E.; Reichmann, M.T.; Leslie, A. Understanding the tuberculosis granuloma: The matrix revolutions. *Trends Mol. Med.* **2022**, *28*, 143–154. [CrossRef] [PubMed]
7. Layre, E. Trafficking of Mycobacterium tuberculosis envelope components and release within extracellular vesicles: Host-pathogen interactions beyond the wall. *Front. Immunol.* **2020**, *11*, 1230. [CrossRef]
8. Abreu, R.; Giri, P.; Quinn, F. Host-pathogen interaction as a novel target for host-directed therapies in tuberculosis. *Front. Immunol.* **2020**, *11*, 1553. [CrossRef] [PubMed]
9. Urbanowski, M.E.; Ordonez, A.A.; Ruiz-Bedoya, C.A.; Jain, S.K.; Bishai, W.R. Cavitary tuberculosis: The gateway of disease transmission. *Lancet Infect. Dis.* **2020**, *20*, e117–e128. [CrossRef]

10. Kathamuthu, G.R.; Kumar, N.P.; Moideen, K.; Nair, D.; Banurekha, V.V.; Sridhar, R.; Baskaran, D.; Babu, S. Matrix metalloproteinases and tissue inhibitors of metalloproteinases are potential biomarkers of pulmonary and extra-pulmonary tuberculosis. *Front. Immunol.* **2020**, *11*, 419. [CrossRef]
11. Yu, Y.; Jiang, X.X.; Li, J.C. Biomarker discovery for tuberculosis using metabolomics. *Front. Mol. Biosci.* **2023**, *10*, 1099654. [CrossRef]
12. Elkington, P.T.; Ugarte-Gil, C.A.; Friedland, J.S. Matrix metalloproteinases in tuberculosis. *Eur. Respir. J.* **2011**, *38*, 456–464. [CrossRef] [PubMed]
13. Sabir, N.; Hussain, T.; Mangi, M.H.; Zhao, D.; Zhou, X. Matrix metalloproteinases: Expression, regulation and role in the immunopathology of tuberculosis. *Cell Prolif.* **2019**, *52*, e12649. [CrossRef] [PubMed]
14. Rohlwink, U.K.; Walker, N.F.; Ordonez, A.A.; Li, Y.J.; Tucker, E.W.; Elkington, P.T.; Wilkinson, R.J.; Wilkinson, K.A. Matrix Metalloproteinases in Pulmonary and Central Nervous System Tuberculosis—A Review. *Int. J. Mol. Sci.* **2019**, *20*, 1350. [CrossRef] [PubMed]
15. Lavrova, A.I.; Esmedljaeva, D.S.; Belik, V.; Postnikov, E.B. Matrix metalloproteinases as markers of acute inflammation process in the pulmonary tuberculosis. *Data* **2019**, *4*, 137. [CrossRef]
16. Nogueira, B.M.F.; Krishnan, S.; Barreto-Duarte, B.; Araújo-Pereira, M.; Queiroz, A.T.L.; Ellner, J.J.; Salgame, P.; Scriba, T.J.; Sterling, T.R.; Gupta, A.; et al. Diagnostic biomarkers for active tuberculosis: Progress and challenges. *EMBO Mol. Med.* **2022**, *14*, e14088. [CrossRef]
17. Kumar, N.P.; Moideen, K.; Nancy, A.; Viswanathan, V.; Thiruvengadam, K.; Sivakumar, S.; Hissar, S.; Nair, D.; Banurekha, V.V.; Kornfeld, H.; et al. Association of Plasma Matrix Metalloproteinase and Tissue Inhibitors of Matrix Metalloproteinase Levels With Adverse Treatment Outcomes Among Patients With Pulmonary Tuberculosis. *JAMA Netw. Open* **2020**, *3*, e2027754. [CrossRef]
18. Postnikov, E.B.; Esmedljaeva, D.S.; Lavrova, A.I. A CatBoost machine learning for prognosis of pathogen's drug resistance in pulmonary tuberculosis. In Proceedings of the 2020 IEEE 2nd Global Conference on Life Sciences and Technologies (LifeTech), Kyoto, Japan, 10–12 March 2020; pp. 86–87. [CrossRef]
19. Lavrova, A.I.; Postnikov, E.B. An Improved Diagnostic of the Mycobacterium tuberculosis Drug Resistance Status by Applying a Decision Tree to Probabilities Assigned by the CatBoost Multiclassifier of Matrix Metalloproteinases Biomarkers. *Diagnostics* **2022**, *12*, 2847. [CrossRef]
20. Leonard-Duke, J.; Evans, S.; Hannan, R.T.; Barker, T.H.; Bates, J.H.T.; Bonham, C.A.; Moore, B.B.; Kirschner, D.E.; Peirce, S.M. Multi-scale models of lung fibrosis. *Matrix Biol.* **2020**, *91*, 35–50. [CrossRef]
21. Ruggiero, S.M.; Pilvankar, M.R.; Ford Versypt, A.N. Mathematical modeling of tuberculosis granuloma activation. *Processes* **2017**, *5*, 79. [CrossRef]
22. Prats, C.; Vilaplana, C.; Valls, J.; Marzo, E.; Cardona, P.J.; López, D. Local inflammation, dissemination and coalescence of lesions are key for the progression toward active tuberculosis: The bubble model. *Front. Microbiol.* **2016**, *7*, 33. [CrossRef]
23. Lin, P.L.; Ford, C.B.; Coleman, M.T.; Myers, A.J.; Gawande, R.; Ioerger, T.; Sacchettini, J.; Fortune, S.M.; Flynn, J.L. Sterilization of granulomas is common in active and latent tuberculosis despite within-host variability in bacterial killing. *Nat. Med.* **2014**, *20*, 75–79. [CrossRef] [PubMed]
24. Minucci, S.; Heise, R.L.; Valentine, M.S.; Gninzeko, F.J.K.; Reynolds, A.M. Mathematical modeling of ventilator-induced lung inflammation. *J. Theor. Biol.* **2021**, *526*, 110738. [CrossRef] [PubMed]
25. Sharebiani, H.; Hajimiri, S.; Abbasnia, S.; Soleimanpour, S.; Asnaashari, A.M.H.; Valizadeh, N.; Derakhshan, M.; Pilpa, R.; Firouzeh, A.; Ghazvini, K.; et al. Game theory applications in host-microbe interactions toward disease manifestation: Mycobacterium tuberculosis infection as an example. *Iran. J. Basic Med. Sci.* **2021**, *24*, 1324–1335. . [CrossRef] [PubMed]
26. Sershen, C.L.; Salim, T.; May, E.E. Investigating the comorbidity of COPD and tuberculosis, a computational study. *Front. Syst. Biol.* **2023**, *3*, 940097. [CrossRef]
27. Lavrova, A.I.; Postnikov, E.B.; Esmedljaeva, D.S. Mathematical modeling of cavity development in lung tuberculosis. *Proc. SPIE* **2021**, *11847*, 1184707. [CrossRef]
28. Bazykin, A.D. *Nonlinear Dynamics of Interacting Populations*; World Scientific: Singapore, 1998.
29. Kryvohuz, M.; Mukamel, S. Nonlinear response theory in chemical kinetics. *J. Chem. Phys.* **2014**, *140*, 034111. [CrossRef]
30. Amaral, E.P.; Vinhaes, C.L.; Oliveira-de Souza, D.; Nogueira, B.; Akrami, K.M.; Andrade, B.B. The interplay between systemic inflammation, oxidative stress, and tissue remodeling in tuberculosis. *Antioxidants Redox Signal.* **2021**, *34*, 471–485. [CrossRef]
31. Kremer, M. Population Growth and Technological Change: One Million B.C. to 1990. *Q. J. Econ.* **1993**, *108*, 681–716. [CrossRef]
32. Markov, A.V.; Korotayev, A.V. Phanerozoic marine biodiversity follows a hyperbolic trend. *Palaeoworld* **2007**, *16*, 311–318. [CrossRef]
33. Holling, C.S. Some Characteristics of Simple Types of Predation and Parasitism. *Can. Entomol.* **1959**, *91*, 385–398. [CrossRef]

34. Ashby, M.T. Appreciating formal similarities in the kinetics of homogeneous, heterogeneous, and enzyme catalysis. *J. Chem. Educ.* **2007**, *84*, 1515. [CrossRef]
35. Weller, S.W. Kinetics of heterogeneous catalyzed reactions. *Catal. Rev.* **1992**, *34*, 227–280. [CrossRef]